

- Fiz. 64, 48 (1973) [Sov. Phys. JETP 37, 28 (1973)].
- ⁷S. W. Hawking, Nature (London) 248, 30 (1974), and "Particle Creation by Black Holes" (to be published).
- ⁸J. M. Bardeen, B. Carter, and S. W. Hawking, Commun. Math. Phys. 31, 161 (1973).
- ⁹J. D. Beckenstein, Phys. Rev. D 7, 2333 (1973).
- ¹⁰D. Christodoulou, Phys. Rev. Lett. 25, 1596 (1970).
- ¹¹L. Smarr, Phys. Rev. Lett. 30, 71 (1973).
- ¹²B. Carter, Phys. Rev. Lett. 26, 331 (1971).
- ¹³D. C. Robinson, "Classification of Black Holes with Electromagnetic Fields" (to be published).
- ¹⁴W. Israel, Phys. Rev. 164, 1776 (1968).
- ¹⁵W. Israel, Commun. Math. Phys. 8, 245 (1968).
- ¹⁶S. W. Hawking, Commun. Math. Phys. 25, 152 (1972).
- ¹⁷S. W. Hawking and G. F. R. Ellis, *The Large Scale Structure of Space Time* (Cambridge Univ. Press, Cambridge, England, 1973).
- ¹⁸H. Muller Zum Hagen, D. C. Robinson, and H. J. Seifert, "Black Holes in Static Vacuum Spacetimes" (to be published).
- ¹⁹R. Kerr, Phys. Rev. Lett. 11, 237 (1963).
- ²⁰E. T. Newman *et al.*, J. Math. Phys. (N. Y.) 6, 918 (1965).
- ²¹B. Carter, Commun. Math. Phys. 10, 280 (1968).
- ²²S. A. Teukolsky, Astrophys. J. 185, 635 (1973).
- ²³R. Hagedorn, Astron. Astrophys. 5, 184 (1970).
- ²⁴R. H. Dicke, Nature (London) 192, 440 (1961).
- ²⁵B. Carter, in "Confrontation of Cosmological Theories with Observation," edited by M. Longair (North-Holland, Amsterdam, to be published), p. 272.
- ²⁶G. W. Gibbons, "Vacuum Polarization and the Spontaneous Loss of Charge by Black Holes" (to be published).
- ²⁷J. A. Wheeler, "Black Hole Chemical Potentials" (to be published).
- ²⁸J. D. Beckenstein, Phys. Rev. D 5, 1239 (1972).
- ²⁹C. Teitelboim, Phys. Rev. D 5, 2941 (1972).
- ³⁰R. H. Dicke, Phys. Rev. 126, 1580 (1962).
- ³¹B. K. Harrison, R. S. Thorne, M. Wakano, and J. A. Wheeler, *Gravitation Theory and Gravitational Collapse* (Chicago Univ. Press, Chicago, Ill., 1965).
- ³²B. Carter, J. Phys. (Paris), Colloq. 34, C7-39 (1973).

Extraction of $R = \sigma_L / \sigma_T$ from Deep Inelastic $e-p$ and $e-d$ Cross Sections*

E. M. Riordan, A. Bodek, M. Breidenbach, † D. L. Dubin, J. E. Elias, ‡ J. I. Friedman, H. W. Kendall, J. S. Poucher, and M. R. Sogard §
Physics Department and Laboratory for Nuclear Science, Massachusetts Institute of Technology, Cambridge, Massachusetts 02139

and

D. H. Coward

Stanford Linear Accelerator Center, Stanford University, Stanford, California 94305
 (Received 16 May 1974)

The quantity $R = \sigma_L / \sigma_T$ is extracted for the proton, deuteron, and neutron from deep inelastic $e-p$ and $e-d$ scattering cross sections measured in recent experiments at Stanford Linear Accelerator Center. For $\omega \leq 5$ the kinematic behavior of νR_p is consistent with scaling, indicative of spin- $\frac{1}{2}$ constituents in a parton model of the proton. We also find that within large statistical errors, R_d and R_n are consistent with being equal to R_p .

We have extracted longitudinal and transverse virtual photoabsorption cross sections σ_L and σ_T from deep inelastic electron-proton ($e-p$) and electron-deuteron ($e-d$) scattering cross sections that were measured in two experiments^{1,2} at the Stanford Linear Accelerator Center (SLAC). Values of $R = \sigma_L / \sigma_T$ for the proton (R_p) are presented and compared with current theoretical predictions. In an earlier experiment,³ R_p was found to be consistent with the constant value 0.18 ± 0.10 . This small value of R_p suggested spin- $\frac{1}{2}$ constituents⁴ of the proton, but full verification of this hypothesis requires a detailed knowledge of its kinematic variation.⁵ In the present work R_p is determined over a larger kinematic range

and its accuracy is sufficiently improved to allow examination of its kinematic variation. The first determinations of R for the deuteron and neutron, R_d and R_n , are also reported.

The inelastic scattering of an electron of incident energy E to final energy E' through an angle θ is described in the first Born approximation by the exchange of a virtual photon of energy $\nu = E - E'$ and invariant mass squared $q^2 = -4EE' \sin^2(\theta/2) = -Q^2$. The differential cross section is related to σ_L and σ_T as follows⁶:

$$\frac{d^2\sigma}{d\Omega dE'}(E, E', \theta) = \Gamma[\sigma_T(\nu, Q^2) + \epsilon\sigma_L(\nu, Q^2)],$$

where Γ is the flux of transverse virtual photons

and $\epsilon = [1 + 2(1 + \nu^2/Q^2) \tan^2(\theta/2)]^{-1}$ is the polarization of the virtual photons. Also, $W = (M^2 + 2M\nu - Q^2)^{1/2}$ is the mass of the unobserved final hadronic state, where M is the proton mass. We use the scaling variable ω defined by $\omega = 1/x = 2M\nu/Q^2$. The quantity R is related to the familiar structure functions W_1 and W_2 by

$$R = \sigma_L/\sigma_T = (W_2/W_1)(1 + \nu^2/Q^2) - 1.$$

Extraction of R and σ_T at fixed (ν, Q^2) requires differential cross sections for at least two values of θ (or ϵ) and is equivalent to separation of W_1 and W_2 .

The inelastic $e-p$ and $e-d$ cross sections were measured with two different single-arm focusing spectrometers in separate experiments to obtain data over a large range of ϵ . The bulk of the cross-section data used in the extraction of R had been measured^{1,7,8} at 18°, 26°, and 34° with the SLAC 8-GeV spectrometer. Incident energies E ranged from 4.5 to 18 GeV; at each incident energy, scattered energies E' ranged from that corresponding to electroproduction threshold down to 1.5 GeV. The measured cross sections consequently spanned triangular regions of (ν, Q^2) space at each angle and permitted interpolations for radiative corrections and for extractions of R . Additional cross sections used in the analysis had been measured in an earlier experiment^{2,9,10} at 6° and 10° with the SLAC 20-GeV spectrometer and a different set of target cells. In that experiment E ranged from 4.5 to 19.5 GeV and E' ranged as low as 2.5 GeV. The analyses⁷⁻⁹ of the raw experimental data from the two experiments were similar and the radiative-correction procedures^{7,9} were identical.

A fit to the elastic $e-p$ cross sections measured at the small angles was on the average 2% lower than the elastic $e-p$ cross sections measured at 18°, 26°, and 34°. Detailed studies⁷ of effects that could alter the elastic and inelastic cross sections differently showed that this 2% difference was also applicable to the inelastic $e-p$ cross sections. Therefore, the 6° and 10° inelastic $e-p$ cross sections¹⁰ were multiplied by the relative normalization factor 1.02 ± 0.02 before the extraction of R_p . An accurate determination of the normalization factor for the inelastic $e-d$ cross sections was not feasible due to the quasi-elastic $e-d$ cross-section uncertainties arising both from the inelastic background subtractions and from corrections due to deuteron binding effects. Therefore, the 6° and 10° $e-d$ data were not used in the extraction of R_d and R_n .

Values of

$$\Sigma(\nu, Q^2, \theta) = \frac{1}{\Gamma} \frac{d^2\sigma}{d\Omega dE'}(\nu, Q^2, \theta)$$

were obtained by interpolation of the $e-p$ cross sections measured at each angle to selected kinematic points (ν, Q^2) that fell within the overlaps of two or more of the five triangles measured in the two experiments. An array of 86 kinematic points with $W > 2$ GeV and $Q^2 > 1$ GeV², chosen to reflect the number and distribution of measured cross sections, was used in a systematic study of the behavior of R_p at fixed ω . For each (ν, Q^2) point, R_p was determined from the slope of a linear least-square fit to values of Σ versus ϵ . Values of R_p are given in Table I along with their statistical errors and estimates of the systematic uncertainty ΔR_p . Because of the interpolations, the value of R_p and its error at any point are correlated with those of neighboring kinematic points. One contribution to ΔR_p at each (ν, Q^2) point arises from uncertainties in the experimental parameters (e.g., E' dependence of the spectrometer acceptance, and fluctuations in the incident beam direction) leading to systematic changes in Σ as a function of θ . This uncertainty ranges from 0.03 to 0.19 in R_p and generally is less than 0.08. Where cross sections from both experiments are used in the extraction of R_p , the 2% uncertainty in the relative normalization factor contributes an uncertainty of typically 0.07 in R_p . A third uncertainty arises from approximations in the radiative corrections and is estimated to range from 0.01 to 0.18 in R_p , with the largest uncertainty occurring at large ω or large ν . For $\omega \leq 5$, however, this uncertainty is believed to be no more than 0.06 in R_p . The systematic uncertainty quoted in Table I is the quadratic sum of the above three uncertainties.

Within parton models, the behavior of νR_p as a function of Q^2 for fixed $\omega = 1/x$ reflects the spin quantum numbers of those charged partons carrying a fraction x of the proton's momentum.^{4,5} If the charged partons have spin- $\frac{1}{2}$, light-cone algebras predict that νR_p should scale^{5,11}; i.e., $\nu R_p = r(\omega)$. If there are some charged spin-0 partons present,¹² then $\nu R_p = a(\omega) + b(\omega)\nu$; here, $b(\omega) = W_2^{(0)}/W_2^{(1/2)}$, where $W_2^{(0)}$ and $W_2^{(1/2)}$ are the contributions to W_2 from spin-0 and spin- $\frac{1}{2}$ partons in the limit of large Q^2 . Figure 1 shows νR_p plotted versus Q^2 for $\omega = 2, 5, \text{ and } 10$; the solid lines represent least-square fits of the form $\nu R_p = a + b\nu = a + (\omega/2M)bQ^2$. Best fit values of b and its statistical error are given in Table II for the ten

TABLE I. Values of R_p listed with statistical errors and estimated systematic uncertainties ΔR_p .

ω	ν (GeV)	Q^2 (GeV) ²	R_p	ΔR_p	ω	ν (GeV)	Q^2 (GeV) ²	R_p	ΔR_p	ω	ν (GeV)	Q^2 (GeV) ²	R_p	ΔR_p
1.5	5.0	6.26	0.11±0.17	0.08	2.5	3.0	2.25	0.20±0.08	0.13	5.0	3.0	1.13	0.40±0.12	0.20
1.5	6.0	7.51	0.05±0.08	0.08	2.5	4.0	3.00	0.16±0.05	0.08	5.0	4.0	1.50	0.48±0.12	0.15
1.5	7.0	8.76	0.64±0.26	0.13	2.5	5.0	3.75	0.17±0.06	0.09	5.0	5.0	1.88	0.20±0.07	0.09
1.5	8.0	10.01	0.76±0.35	0.17	2.5	6.0	4.50	0.14±0.06	0.07	5.0	6.0	2.25	0.15±0.07	0.09
1.5	9.0	11.26	0.12±0.18	0.09	2.5	7.0	5.25	0.08±0.06	0.08	5.0	7.0	2.63	0.16±0.07	0.08
1.5	10.0	12.51	-0.10±0.15	0.06	2.5	8.0	6.00	0.03±0.06	0.06	5.0	8.0	3.00	0.18±0.09	0.11
1.5	12.0	15.01	0.26±0.58	0.18	2.5	9.0	6.76	0.22±0.14	0.07	5.0	9.0	3.38	0.30±0.13	0.14
					2.5	10.0	7.51	0.26±0.18	0.07	5.0	10.0	3.75	0.18±0.12	0.12
1.75	4.0	4.29	0.04±0.09	0.07	2.5	11.0	8.26	0.25±0.27	0.12	5.0	11.0	4.13	0.12±0.12	0.11
1.75	5.0	5.36	0.22±0.08	0.08	2.5	12.0	9.01	0.01±0.20	0.09					
1.75	6.0	6.43	0.14±0.07	0.08						6.0	4.0	1.25	0.52±0.15	0.18
1.75	7.0	7.51	0.32±0.16	0.08	3.0	3.0	1.88	0.05±0.06	0.10	6.0	5.0	1.56	0.14±0.09	0.10
1.75	8.0	8.58	0.01±0.14	0.06	3.0	4.0	2.50	0.18±0.06	0.08	6.0	6.0	1.88	0.22±0.09	0.10
1.75	9.0	9.65	-0.05±0.15	0.06	3.0	5.0	3.13	0.14±0.05	0.07	6.0	7.0	2.19	0.33±0.09	0.11
1.75	10.0	10.72	-0.03±0.13	0.06	3.0	6.0	3.75	0.01±0.06	0.08	6.0	8.0	2.50	0.41±0.10	0.12
1.75	12.0	12.87	0.09±0.45	0.15	3.0	7.0	4.38	0.13±0.08	0.09	6.0	9.0	2.82	0.41±0.14	0.15
					3.0	8.0	5.00	0.08±0.09	0.08	6.0	10.0	3.13	0.24±0.13	0.13
2.0	4.0	3.75	0.07±0.06	0.07	3.0	9.0	5.63	0.08±0.07	0.08	6.0	11.0	3.44	0.12±0.13	0.12
2.0	5.0	4.69	0.12±0.06	0.08	3.0	10.0	6.26	0.63±0.34	0.16	6.0	12.0	3.75	0.09±0.16	0.11
2.0	6.0	5.63	0.18±0.08	0.07	3.0	11.0	6.88	0.40±0.34	0.13					
2.0	7.0	6.57	0.08±0.07	0.06	3.0	12.0	7.51	0.22±0.26	0.12	7.5	5.0	1.25	0.15±0.10	0.09
2.0	8.0	7.51	-0.08±0.10	0.05						7.5	6.0	1.50	0.17±0.09	0.09
2.0	9.0	8.44	-0.08±0.13	0.05	4.0	3.0	1.41	0.23±0.07	0.12	7.5	7.0	1.75	0.35±0.10	0.11
2.0	10.0	9.38	0.02±0.15	0.06	4.0	4.0	1.88	0.31±0.10	0.13	7.5	8.0	2.00	0.59±0.15	0.13
2.0	11.0	10.32	0.20±0.15	0.07	4.0	5.0	2.35	0.26±0.08	0.10	7.5	9.0	2.25	0.61±0.16	0.13
2.0	12.0	11.26	0.47±0.60	0.20	4.0	6.0	2.82	0.22±0.06	0.10	7.5	10.0	2.50	0.26±0.18	0.14
					4.0	7.0	3.28	0.16±0.08	0.10	7.5	11.0	2.75	0.19±0.17	0.13
					4.0	8.0	3.75	0.10±0.10	0.09	7.5	12.0	3.00	0.21±0.23	0.14
					4.0	9.0	4.22	0.06±0.09	0.08					
					4.0	10.0	4.69	0.01±0.08	0.08	10.0	6.0	1.13	0.16±0.11	0.09
					4.0	11.0	5.16	0.57±0.48	0.16	10.0	7.0	1.31	0.30±0.14	0.10
										10.0	8.0	1.50	0.35±0.14	0.10
										10.0	9.0	1.69	0.32±0.15	0.10
										10.0	10.0	1.88	0.35±0.16	0.10
										10.0	11.0	2.06	0.58±0.31	0.20
										10.0	12.0	2.25	1.03±0.57	0.26

values of ω studied. The three effects leading to the aforementioned uncertainties in R_p also give uncertainties in b ; the systematic uncertainty Δb is the quadratic sum of these three uncertainties. For $\omega \leq 5$ the slope b is small and consistent with zero, indicative of predominantly spin- $\frac{1}{2}$ partons. Over this range of ω , we get a 2 standard deviation upper limit of 20% for the contribution of spin-0 partons to W_2 . For $\omega > 5$, b may be different from zero, but the data for these ω lie in a small range of low Q^2 and a nonzero slope might reflect only the low- Q^2 threshold behavior of R_p .

We have made a number of least-square fits to the 86 values of R_p listed in Table I. A constant value of R_p provides a better fit to the data than $R_p = Q^2/\nu^2$ or the simple vector-dominance¹³ forms $K_p = cQ^2$ or $R_p = cQ^2(1-x)^2$. We obtain R_p

TABLE II. Best fit values of the coefficient b and their statistical errors from least-square fits of the form $\nu R_p = a + b\nu$. Also given are the estimated systematic uncertainties Δb and average values of $\delta = R_d - R_p$ for the range $1.5 \leq \omega \leq 5.0$ where these data are available. Only statistical errors in δ are given.

ω	b	Δb	δ
1.5	0.11±0.28	0.14	-0.09±0.09
1.75	0.02±0.15	0.08	0.08±0.07
2.0	0.04±0.10	0.06	0.13±0.06
2.5	0.03±0.07	0.06	0.04±0.06
3.0	0.12±0.07	0.07	-0.01±0.08
4.0	0.02±0.07	0.06	-0.25±0.12
5.0	0.02±0.09	0.08	-0.20±0.21
6.0	0.20±0.13	0.12	...
7.5	0.66±0.19	0.17	...
10.0	0.80±0.31	0.18	...

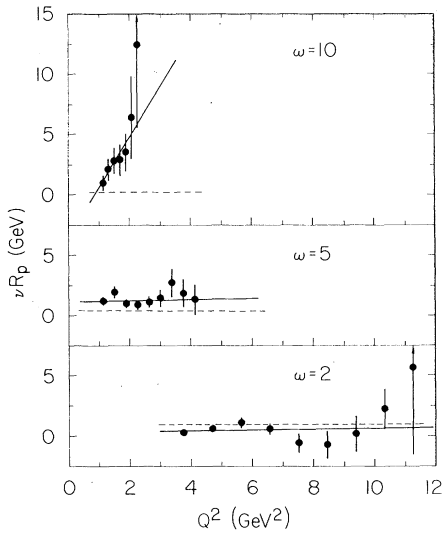


FIG. 1. Values of νR_p plotted with their statistical errors versus Q^2 for fixed values of ω . The solid lines represent least-square fits of the form $\nu R_p = a + b\nu = a + (\omega/2M) bQ^2$, and the dashed lines represent $R_p = Q^2/\nu^2$.

$= 0.16 \pm 0.01$ ($\chi^2 = 138$) with an estimated systematic error of ± 0.09 . An even better fit is obtained with the form¹² $R_p = f(\omega)Q^2/\nu^2$, where $f(\omega) = g\omega^2$ or, equivalently, $R_p = 4gM^2/Q^2$. The best fit coefficient is $g = 0.13 \pm 0.01$ ($\chi^2 = 110$) with an estimated systematic error of ± 0.06 . This deviation from simple Q^2/ν^2 behavior at large ω , predicted from Regge arguments¹² in the framework of light-cone algebras⁵ and deduced¹³ from ρ -electroproduction data,¹⁴ is apparent in Fig. 1 where the dashed lines represent $R_p = Q^2/\nu^2$.

Since only 18° , 26° , and 34° $e-d$ data were used in the analysis, R_d and R_n are less well known than R_p . The quantity $\delta = R_d - R_p$ was extracted at each of the (ν, Q^2) points where interpolated cross sections at two or more of these angles were available. This quantity is determined⁷ from the slope of the ratio of deuteron-to-proton cross sections, σ_d/σ_p , plotted versus $\epsilon' = \epsilon(1 + \epsilon R_p)^{-1}$, and is insensitive to the choice of R_p . The major systematic uncertainties disappear in this ratio⁸ and the uncertainties in δ are predominantly statistical. The extracted values of δ are everywhere consistent with zero, within large statistical errors. Values of δ averaged over Q^2 at fixed ω are presented in Table II. The value

of δ averaged over the full kinematic range $1.5 \leq \omega \leq 5.0$ is 0.02 ± 0.03 . It can be shown⁸ that $R_d = R_p$ implies $R_n = R_p$ and therefore, within the experimental errors, R_d and R_n are consistent with being equal to R_p .

We acknowledge helpful discussions with R. Jaffe and are grateful for programming assistance from E. Miller and R. Verdier.

*Work supported in part by the U.S. Atomic Energy Commission under Contracts No. AT(11-1)-3069 and No. AT(04-3)-515.

†Present address: Stanford Linear Accelerator Center, Stanford University, Stanford, Calif. 94305.

‡Present address: National Accelerator Laboratory, Batavia, Ill. 60510.

§Present address: Laboratory of Nuclear Studies, Cornell University, Ithaca, N.Y. 14850.

¹A. Bodek *et al.*, Phys. Rev. Lett. **30**, 1087 (1973).

²J. S. Poucher *et al.*, Phys. Rev. Lett. **32**, 118 (1974), and SLAC Report No. SLAC-PUB-1309 (unpublished).

³G. Miller *et al.*, Phys. Rev. D **5**, 528 (1972).

⁴C. G. Callan and D. J. Gross, Phys. Rev. Lett. **22**, 156 (1969).

⁵J. E. Mandula, Phys. Rev. D **8**, 328 (1973).

⁶L. N. Hand, Phys. Rev. **129**, 1834 (1963).

⁷E. M. Riordan, Ph.D. thesis, Massachusetts Institute of Technology, 1973, available as Report No. LNS-COO-3069-176 (unpublished).

⁸A. Bodek, Ph.D. thesis, Massachusetts Institute of Technology, 1972, available as Report No. LNS-COO-3069-116 (unpublished).

⁹J. S. Poucher, Ph.D. thesis, Massachusetts Institute of Technology, 1971 (unpublished).

¹⁰This experiment was performed by a collaboration between Massachusetts Institute of Technology and SLAC Group A. The cross sections used in the extractions of R were taken from the MIT analysis of this data. Because of differences in radiative-correction methods, these cross sections were typically 1.5% lower than those reported in Ref. 2.

¹¹R. P. Feynman, *Photon-Hadron Interactions* (Benjamin, New York, 1972).

¹²J. F. Gunion and R. L. Jaffe, Phys. Rev. D **8**, 3215 (1973).

¹³J. J. Sakurai, Phys. Rev. Lett. **22**, 981 (1969), and **30**, 245 (1973).

¹⁴For a review of ρ -electroproduction data, see the talk by K. Berkelman, in *Proceedings of the Sixteenth International Conference on High Energy Physics, The University of Chicago and National Accelerator Laboratory, 1972*, edited by J. D. Jackson and A. Roberts (National Accelerator Laboratory, Batavia, Ill., 1973), Vol. 4, p. 41.